High-Performance CW 1.26-μm GaInNAsSb–SQW Ridge Lasers

Hitoshi Shimizu, Kouji Kumada, Seiji Uchiyama, *Member, IEEE*, and Akihiko Kasukawa, *Associate Member, IEEE*

***Abstract*—Long wavelength GaInNAsSb–SQW lasers and GaInAsSb–SQW lasers that include a small amount of Sb were successfully grown by gas-source molecular beam epitaxy (GSMBE). We confirmed that Sb reacts in a highly strained GaInAs–GaAs system and GaInNAs–GaAs system like a surfactant, which increases the critical thickness at which the growth mode changes from two-dimensional (2-D) growth to three-dimentional (3-D) growth. The lasers were processed into ridge lasers. The GaInNAsSb lasers oscillated under continuous-wave (CW) operation at 1.258 μm at room temperature. The low CW threshold current of 12.4 mA and high characteristic temperature (T_0) of 157 K were obtained for GaInNAsSb lasers, which is the best result for GaInNAs-based narrow stripe lasers. Further, the GaInNAsSb laser oscillated under CW conditions over 100°C. On the other hand, GaInAsSb lasers oscillated under CW operation at 1.20 μm at room temperature. The low CW threshold current of 6.3 mA and high characteristic temperature (T_0) of 256 K were obtained for GaInAsSb lasers, which is also the best result for 1.2-μm-range highly strained GaInAs-based narrow stripe lasers. We can say that GaInNAsSb lasers are very promising material for a realizing pertier-free access network. Further, the differential gain of GaInNAs-based SQW lasers was estimated for the first time. GaInNAsSb–SQW lasers have the extremely large differential gain of 1.06×10^{-15} cm^2 in spite of the single-QW lasers; therefore, GaInNAsSb lasers are also suitable for high-speed lasers in the long wavelength region.**

***Index Terms*—Communication systems, epitaxial growth, GaInNAs, highly strained, quantum-well lasers, ridge laser, Sb, surfactant.**

I. Introduction

LONG WAVELENGTH lasers emitting at 1.2∼1.3 μm grown on GaAs substrates have been attracting much interest. GaInNAs [1]–[9], GaInAs quantum film (QF) [3], [10]–[12], GaAsSb [13], and InAs quantum dots (QD) [14], [15] have been reported to realize this wavelength on GaAs substrates. Among the candidates, the large conduction band offset can be realized for GaInNAs and highly strained GaInAs QF, which leads to the strong electron confinement in the wells and leads to the high characteristic temperature (T_0). The large T_0 of 127–274 K [1], [4], [7], [10], which are much larger than the conventional long-wavelength GaInAsP–InP system, have been reported in these materials. Therefore, a peltier-free system with low cost for access network can be realized by using GaInNAs or highly strained GaInAs QF lasers. Further, there are the advantages for the long-wavelength vertical cavity surface emitting laser (VCSEL) on GaAs substrates that it can be grown monolithically on a GaAs–AlGaAs DBR mirror with high reflectivity and high thermal conductivity, and it can utilize the mature technology of 850–980-nm VCSELs such as AlAs selective oxidation [16].

However, most published results referred to broad area laser characteristics with respect to GaInNAs and highly strained GaInAs QW lasers and there were few results on narrow stripe lasers so far. The large T_0 (148–204 K) were reported on narrow stripe GaInNAs lasers [4], but the threshold currents (Ith) were very high (75–500 mA) [2], [4]. Recently, GaInNAs lasers with low threshold current at room temperature ($Ith = 11$ mA) were reported [6], but this laser has the relatively low T_0 of 70–80 K [6].

To obtain the 1.3-μm-GaInNAs lasers with the good crystalline quality, 1.2-μm-range GaInAs QF lasers that have the strong photoluminescence intensity have to be grown because nitride makes the photoluminescence intensity poor.

A few of 1.2-μm-range GaInAs QF lasers were reported by MOCVD growth [3], [10]–[12]. Although the photoluminescence up to 1.224 μm were reported [17], 1.2-μm-range GaInAs QF lasers have not been reported by MBE growth. GaInAs QF lasers grown by MBE were only limited to around 1.12 μm [18] because the longer migration length in MBE-growth is apt to cause the growth of QD in a highly strained GaInAs–GaAs system [14], [15]. The QF with a higher indium composition would be realized with good crystalline quality by using a high growth rate, a low growth temperature, a high V/III pressure ratio, and a surfactant [19]. With respect to surfactants, only Te has been reported so far as the surfactant for the GaInAs–GaAs system [20]. On the other hand, Sb is reported as a surfactant in Si–Ge system and the GaInNAs system [8].

In this paper, we investigated highly strained GaInAs QF and GaInNAs QF lasers that include a small amount of Sb like a surfactant on the GaAs substrates to improve the crystalline-quality by gas-source molecular-beam epitaxy (GSMBE) growth; we studied the performance of GaInAsSb and GaInNAsSb–SQW ridge lasers. In Section II, we discuss the effect of Sb on the photoluminescence characteristics of GaInAsSb and GaInNAsSb SQW. The lasing wavelength of GaInAsSb QF lasers was increased up to 1.185 μm to keep the low threshold current density of as low as 280 A/cm^2 [21], which is one of the lowest ever reported for 1.2-μm-range GaInAs-based QF lasers. In Section III, we fabricated ridge lasers and extracted the basic laser parameters such as gain coefficient, internal loss, and characteristic temperature. We report the high performance continuous-wave (CW) lasing characteristics of 1.26-μm-GaInNAsSb–SQW lasers ($Ith = 12.4$ mA at 25 °C, $T_0 = 157$ K) and 1.20-μm-GaInAsSb–SQW lasers

Manuscript received October 12, 2000; revised March 8, 2001.

The authors are with Furukawa Electric Co., Ltd., Yokohama Research and Development Laboratories, 220-0073 Yokohama, Japan (e-mail: shimizu@yokoken.furukawa.co.jp).

Publisher Item Identifier S 1077-260X(01)08009-1.

($Ith = 6.3$ mA at 20 °C, $T_0 = 256$ K). Further, the differential gain of GaInNAs-based SQW lasers was estimated for the first time. The extremely large differential gain of 1.06×10^{-15} cm^2 was estimated in spite of the single-QW lasers.

II. Growth of SQW Lasers and Evaluation of Basic Material Quality

A. Growth Conditions of GaInAsSb–SQW

First of all, we studied 1.2-μm-range highly strained $Ga_{0.61}In_{0.39}As_ySb_{1-y}$-GaAs–SQW lasers on n-(100) just GaAs substrates by GSMBE in which group V was supplied by AsH_3 and PH_3, group III was supplied by metal In and Ga, and Sb was supplied by solid source. The lasers consisted of n-, p-GaInP cladding, a highly strained SQW active layer (7.3 -nm thick), and 130-nm-thick GaAs SCH layers located on both sides of SQW layer.

We calculated the critical thickness using Matthews and Blakeslee's formula [22] against indium composition in GaInAs film on GaAs substrates. We designed the composition of In in GaInAs film as 39% to increase the wavelength. As $Ga_{0.61}In_{0.39}As$–GaAs QF has an extremely high compressive strain of 2.8%, the calculated critical thickness was only 4 nm. However, we set the thickness of QF to 7.3 nm by taking into account the increasing wavelength. The low growth temperature in GSMBE can accommodate the thick QW exceeding the critical thickness, and adding Sb like a surfactant in highly strained material can help exceeding the critical thickness. The growth temperature of the active and cladding layers was set to 440 °C and 460 °C, respectively; the pressure of AsH_3 controlled by baratron was set to 9×10^{-5} torr and the growth rate of the well layer which is determined by the total flux of group III was set to 2.1 μm/h. By adding Sb during the growth of the well layer, we investigated the photoluminescence (PL) characteristics' dependence on the flux of Sb. Fig. 1 shows PL intensity and PL wavelength against the flux of Sb. From this figure, we can see that Sb is very effective to improve the crystalline quality by prohibiting the three-dimensional (3-D) growth like a surfactant in the highly strained GaInAs–GaAs QF and that PL intensity increases most efficiently with the Sb flux of 2×10^{-7} torr. The PL intensity of $Ga_{0.61}In_{0.39}AsSb$ with Sb flux of 2×10^{-7} torr ($\lambda = 1.17$ μm) is about one-fourth as strong as that of $Ga_{0.65}In_{0.35}As$ QF ($\lambda = 1.12$ μm).

To study the incorporation rate of Sb into the film, we grew GaAsSb, whose growth rates, AsH_3 pressure, and growth temperature, were set to the same condition as the GaInAsSb well layer. Fig. 2 shows the relationship between Sb composition determined by X-ray diffraction on GaAsSb film and the flux of Sb. Sb was incorporated into the film with the linearity up to the 5×10^{-6} torr. The calculated wavelength of GaInAsSb SQW, where the incorporation rate of Sb is assumed to be identical to that of GaAsSb, was also shown in Fig. 1. Here, the bulk energy gap of $GaAs_ySb_{1-y}$ [23] and the bulk energy gap of $InAs_ySb_{1-y}$ [23] without strain effect were reported to have the relationship at room temperature as follows:

$$E_g(GaAs_ySb_{1-y}) = 0.726 - 0.502y + 1.2y^2 \quad (1)$$

$$E_g(InAs_ySb_{1-y}) = 0.18 - 0.41y + 0.58y^2. \quad (2)$$

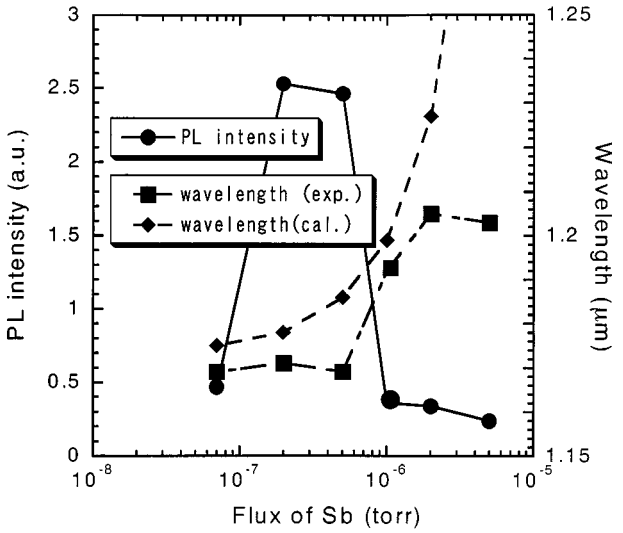

Fig. 1. PL intensity and PL wavelength against Sb flux for GaInAsSb–GaAs SQW. The calculated wavelength where the incorporation rate of Sb is identical to that of GaAsSb was also shown.

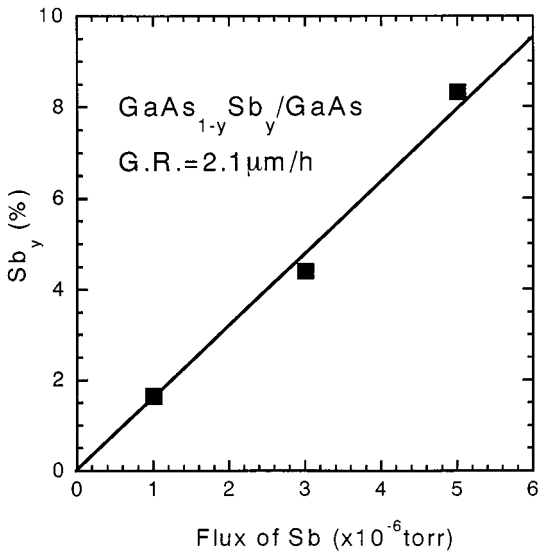

Fig. 2. Sb composition against Sb flux in GaAsSb on GaAs.

The bulk energy gap of $Ga_xIn_{1-x}As_ySb_{1-y}$ without strain effect can be obtained from these two materials by Vegard's rule as follows:

$$\begin{aligned} &E_g(Ga_xIn_{1-x}As_ySb_{1-y}) \\ &\quad = E_g\{(GaAs_ySb_{1-y})_x(InAs_ySb_{1-y})_{1-x}\} \\ &\quad = xE_g(GaAs_ySb_{1-y}) + (1-x)E_g(InAs_ySb_{1-y}) \\ &\quad = x(0.726 - 0.502y + 1.2y^2) \\ &\qquad + (1-x)(0.18 - 0.41y + 0.58y^2). \end{aligned} \quad (3)$$

The conduction band offset was assumed to be $\Delta E_c = 0.7\Delta E_g$ in the calculation. The calculated wavelength agrees relatively well with the experimental data up to an Sb flux of 2×10^{-6} torr. With the Sb flux of 2×10^{-7} torr where PL intensity becomes the largest, the composition can be estimated as

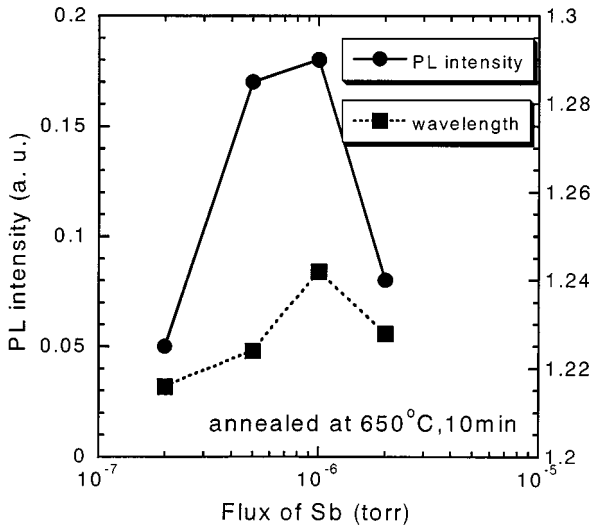

Fig. 3. PL intensity and PL wavelength against Sb flux for GaInNAsSb–GaAs SQW.

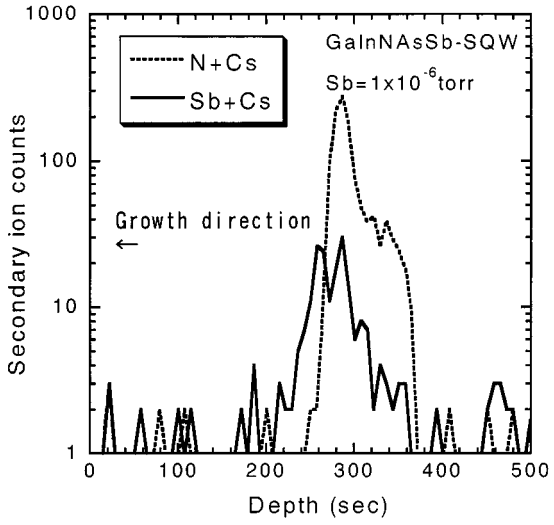

Fig. 4. SIMS profile for GaInNAsSb–SQW lasers with Sb flux of 1×10^{-6} torr, where N signals (Cs + N ion) and Sb signals (Cs + Sb ion) were shown.

$Ga_{0.61}In_{0.39}As_{0.9968}Sb_{0.0032}$. Therefore, Sb does not react as a surfactant exactly but reacts as a surfactant-like because it is incorporated slightly into the film to improve the crystalline quality. Sb seems to lower the surface-free energy and suppress the surface diffusion, which leads to prohibiting the island formation [8], [19]. So far, Te has been reported as a surfactant for the GaInAs–GaAs system [20]. We confirmed for the first time that Sb reacts in a highly strained GaInAs–GaAs system like a surfactant, which increases the critical thickness at which the growth mode changes from two–dimensional (2-D) growth to 3-D growth [21]. These are discussed again in the Section II-B by observing the transmission electron microscopy (TEM) image.

With the Sb flux of 5×10^{-6} torr, the composition of Sb and the amount of strain become 8% and 3.41%, respectively. The reason why the calculated wavelength does not agree with the experimental data with Sb flux of more than 5×10^{-6} torr and why the PL intensity decreases for this amount of Sb could be due to the misfit dislocation and/or the existence of miscibility gap in GaInAsSb.

B. Growth Conditions of GaInNAsSb–SQW

Next, we studied GaInNAsSb–SQW lasers grown by GSMBE, where the N source is N radical generated by an RF plasma cell. The lasers consisted of the same structures as GaInAsSb lasers except for composing the well layer with the GaInNAsSb–SQW layer. The growth temperature of the active layer and cladding layer was set to 460 °C, the flux of AsH_3 controlled by baratron was set to 9×10^{-5} torr, the growth rate of the well layer which is determined by the total flux of group III was set to 2.1 μm/h, and the flow rate of N_2 was fixed at 0.05 ccm. To recover the crystalline quality of the GaInNAsSb layer, the lasers were annealed after the growth at 650 °C for 10 min in the atmosphere of N_2 flow. The lasers were capped by GaAs substrates to prevent the phosphorus atoms from decomposing from the surface of epitaxial layer. We investigated the effect of Sb on the PL characteristics. Fig. 3 shows the PL intensity and PL wavelength against the flux of Sb. With the Sb flux of 1×10^{-6} torr, where PL intensity becomes the largest, the composition of SQW can be estimated as $Ga_{0.61}In_{0.39}N_{1-y-0.016}As_ySb_{0.016}$ from the estimation in Fig. 2. PL intensity of $Ga_{0.61}In_{0.39}N_{1-y-0.016}As_ySb_{0.016}$ with Sb flux of 1×10^{-6} torr ($\lambda = 1.24$ μm) is about 1/20 as strong as that of $Ga_{0.65}In_{0.35}As$ QF ($\lambda = 1.12$ μm). The wavelengths of as-grown $Ga_{0.61}In_{0.39}As_{0.984}Sb_{0.016}$ and as-grown $Ga_{0.61}In_{0.39}N_{1-y-0.016}As_ySb_{0.016}$ were 1.19 and 1.27 μm, respectively. We estimated the N composition as 0.44% from the wavelength shift of 80 nm. The FWHM of GaInNAsSb–SQW was 23 meV, which is almost the same value as $Ga_{0.61}In_{0.39}AsSb$–SQW lasers (19 meV). At the growth condition without Sb, the FWHM becomes over 200 meV at room temperature in this composition, so we can say that Sb is very effective to suppress the 3-D growth in this material.

To investigate the crystalline characteristics of GaInNAsSb–SQW laser further, we studied the secondary ion mass spectroscopy (SIMS) and TEM for the film with a variety of Sb amounts. Fig. 4 shows SIMS for GaInNAsSb–SQW lasers with an Sb flux of 1×10^{-6} torr, where N signals (Cs + N ion) and Sb signals (Cs + Sb ion) were shown. We calculated the integral intensity of the SIMS signal from this figure and showed the relationship between the integrated intensity of Sb and N amounts and the flux of Sb in Fig. 5. Sb was incorporated into the GaInNAsSb–SQW layer with linearity up to the Sb flux of 2×10^{-6} torr, while the amount of N was almost a constant value.

Fig. 6 shows TEM images for GaInNAsSb-SQW lasers with Sb fluxes of 2×10^{-7} and 1×10^{-6} torr, respectively. The SQW with an Sb flux of 2×10^{-7} torr shows 3-D growth; however, the SQW with Sb flux of 1×10^{-6} torr shows 2-D growth. Sb seems to react in a GaInNAs–GaAs system as well as in a GaInAs–GaAs system like a surfactant, which restricts the formation of 3-D growth by suppressing the surface diffusions, which are caused by lowering the surface-free energy [8], [19].

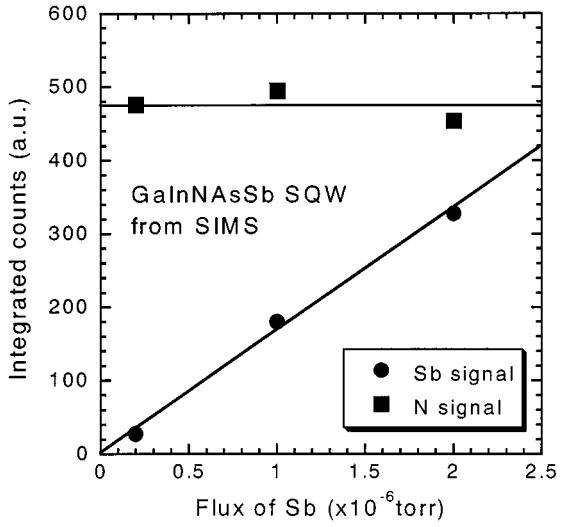

Fig. 5. The integrated intensity of Sb and N in a SIMS profile against the flux of Sb.

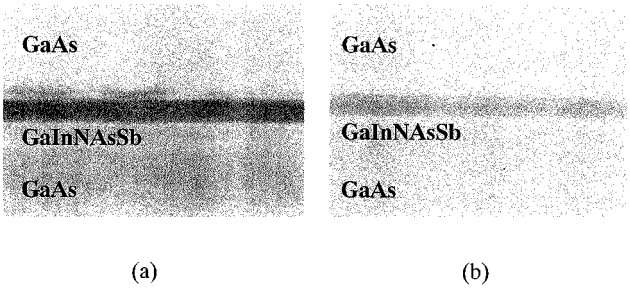

Fig. 6. TEM images for GaInNAsSb–SQW lasers with Sb flux of (a) 2×10^{-7} torr and (b) 1×10^{-6} torr, respectively.

PL intensities decrease with the Sb flux of more than 2×10^{-6} torr. The reason why the PL intensity decreases for this amount of Sb could be due to the defects caused by increasing the strain.

Next, we studied the effect of annealing on the PL characteristics for GaInNAsSb-SQW lasers, where the N composition was decreased to 0.33% by decreasing the N radical, that is, $Ga_{0.61}In_{0.39}N_{0.0033}As_{0.9807}Sb_{0.016}$-SQW as shown in Fig. 7. The increase of PL intensity and the blue shift by annealing were observed as reported in other papers. The annealing temperature of 550 °C almost recovered the quality of GaInNAsSb lasers and the wavelength of the lasers annealed at 550 °C was 1.23 μm and the FWHM of the PL spectrum was as narrow as 23 meV.

C. The Evaluation of Broad Contact Lasers

The threshold current density (J_{th}) and the lasing wavelength were evaluated using broad area lasers for $Ga_{0.61}In_{0.39}As_{0.9968}Sb_{0.0032}$ and $Ga_{0.61}In_{0.39}N_{0.0033}As_{0.9807}Sb_{0.016}$ SQW lasers. The lasing spectrums were 1.185 and 1.246 μm, respectively, for the lasers with a 600-μm cavity at pulse conditions as shown in Fig. 8(a) and (b). The lasing wavelength is the longest value ever reported for an MBE-grown GaInAs–GaAs–QF-based system to our best knowledge [18]. Fig. 9 shows Jth against inverse cavity length. Jth for the lasers with a 900-μm cavity was as low as 280 A/cm^2 for GaInAsSb lasers and 700 A/cm^2 for GaInNAsSb lasers, respectively, which are relatively low

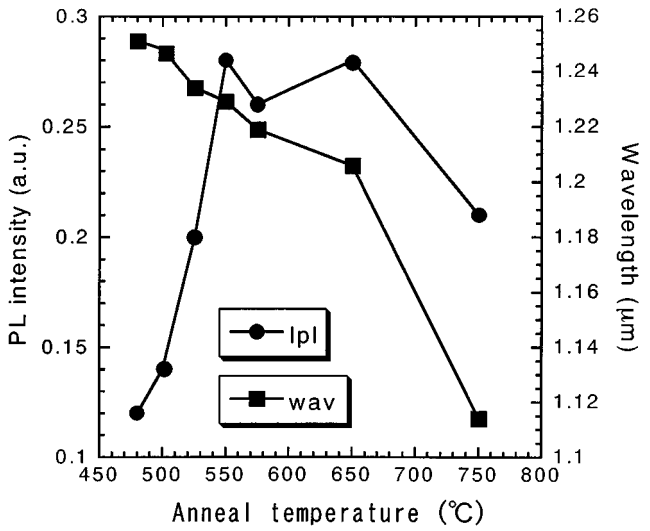

Fig. 7. The effect of annealing on the PL intensities and PL wavelength for GaInNAsSb-SQW lasers, where N composition was decreased to 0.33%.

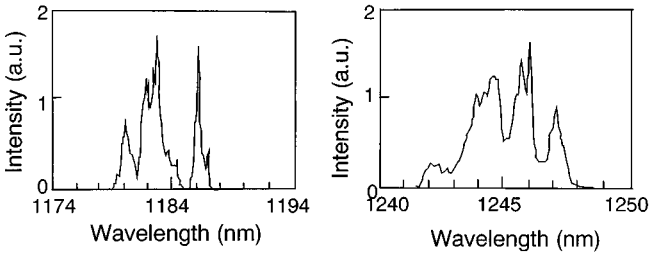

Fig. 8. The lasing spectrum for the broad contact lasers with a 600-μm cavity for (a) a GaInAsSb–SQW laser and (b) a GaInNAsSb–SQW laser.

values among the reported results for 1.2-μm-range GaInAs QF lasers [3], [11], [12] and 1.25–1.3-μm-range GaInNA lasers [1]–[9]. Jth can be expressed as follows [24]:

$$Jth = \frac{N_w J_{tr}}{\eta} \exp\left(\frac{\alpha_i + \frac{1}{2L}\ln\left(\frac{1}{R_f R_r}\right)}{N_w \xi_w G_0}\right) \tag{4}$$

where

J_{tr}	transparent current density;
N_w	number of the well;
η	spontaneous emission efficiency at the threshold;
α_i	internal loss;
L	cavity length;
R_f	reflectivity of the front facet;
R_r	reflectivity of the rear facet;
ξ_w	optical confinement factor per well;
G_0	gain coefficient.

The refractive index (n_r) for 1.185- and 1.246-μm-light can be calculated as 3.47 and 3.46 for GaAs and 3.18 and 3.17 for GaInP. So the optical confinement factor can be obtained by solving the Maxwell's equation as 1.99% for GaInAsSb lasers and 1.98% for GaInNAsSb lasers, respectively, assuming that n_r for GaInAsSb and GaInNAsSb is 3.52. Gain coefficient for GaInAsSb lasers and GaInNAsSb lasers assuming the

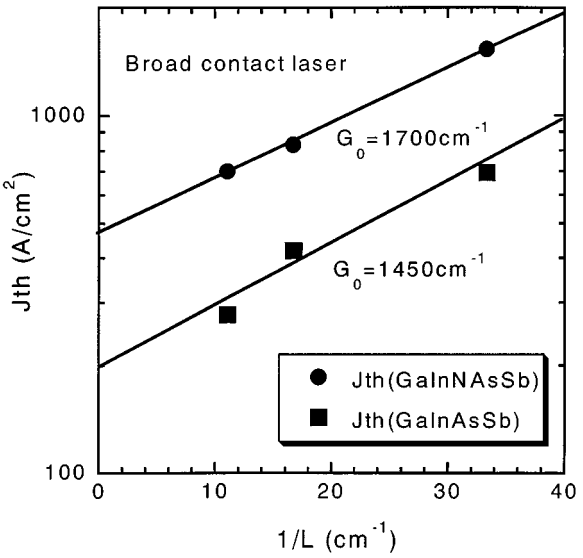

Fig. 9. Jth against inverse cavity length for broad contact lasers of GaInAsSb and GaInNAsSb–SQW lasers.

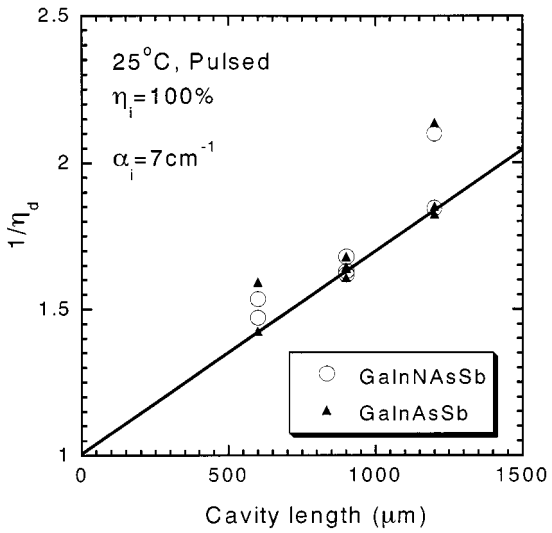

Fig. 10. The inverse external differential quantum efficiency against the cavity length for GaInAsSb and GaInNAsSb–SQW lasers.

logarithmic gain can be estimated as 1450 cm^{-1} and 1700 cm^{-1} by fitting the experimental data in Fig. 9. G_0 of the GaInNAsSb laser is about 1.2 times larger than that of the GaInAsSb laser, which is probably due to the strong electron confinement by the deeper band offset for electrons by adding N; therefore, GaInNAsSb lasers can expect the larger T_0 as compared with GaInAsSb lasers.

III. Lasing Characteristics of Ridge Lasers

We have fabricated ridge lasers with a reverse mesa structure. The off-ridge was etched by the selective wet etching using the interface between n-InGaP cladding and the GaAs optical confinement layer by using the SiN_x mask. The mixture solution of tartaric acid and hydrogen peroxide was used to etch the GaAs layers and the hydrochloric acid was used to etch the GaInP layers. The widths at the bottom of the ridge were about 4.3 μm for both types of lasers.

A. The Evaluation of Threshold Current and Laser Parameters

The internal loss (α_i) and the internal efficiency (η_i) were evaluated from the cavity length dependency of the external differential quantum efficiency for GaInAsSb and GaInNAsSb lasers as shown in Fig. 10. From Fig. 10, α_i and η_i were estimated as 7 cm^{-1} and 100% for both types of the lasers. J_{tr}/η can be solved as 150 A/cm^2 for GaInAsSb lasers and 380 A/cm^2 for GaInNAsSb lasers, respectively, by fitting the experimental results in Fig. 9 by substituting α_i into (4). J_{tr}/η of GaInNAsSb lasers is about 2.5 times larger than that of GaInAsSb lasers mainly because of the poor spontaneous emission efficiency (η) of GaInNAsSb lasers. The further optimization of GaInNAsSb QW growth conditions will improve the value of η, which results in the further reduction of the Jth of GaInNAsSb lasers. The estimated material parameters with respect to GaInAsSb and GaInNAsSb lasers were summarized in Table I.

The experimental Ith for GaInAsSb lasers and GaInNAsSb lasers were plotted in Figs. 11 and 12, respectively, along with the theoretical curves as the function of facet reflectivity. The threshold current (Ith) of the ridge lasers can be expressed as follows [25]:

$$Ith = WL\frac{N_w J_{tr}}{\eta}\exp\left(\frac{\alpha_i + \dfrac{1}{2L}\ln\left(\dfrac{1}{R_f R_r}\right)}{\xi_w N_w G_0}\right) + I_1 L + I_2 \tag{5}$$

where W is the width at the bottom of the ridges, and $I_1 L + I_2$ is the leakage current, in which I_1 and I_2 are the constant values. We referred to the values of I_1 and I_2 reported previously in the analysis of 980-nm-InGaAs–AlGaAs–SQW ridge lasers [25]. The I_2 value was set to the same value as the one reported in the paper ($I_2 = 0.78$ mA) [25]. I_1 was determined by fitting the experimental threshold currents of the lasers with cleaved facets ($L = 300$, 600, 900 μm). I_1 were determined as 1.3×10^{-2}mA/μm for GaInAsSb lasers and 2×10^{-2} mA/μm for GaInNAsSb lasers. Ith values for GaInAsSb were 12.5, 20, and 26 mA for the cavity length of 300, 600, and 900 μm, respectively, by pulse operation at 25 °C. Ith values for GaInNAsSb were 25, 35, and 47 mA for the cavity length of 300, 600, and 900 μm, respectively, by pulse operation at 25 °C. The minimum Ith of the short cavity lasers ($L = 200$ μm) with high reflectivity (HR) coatings on both facets (SiO_2/α–Si; 78%/95%) exhibit as low as 6 and 9.5 mA for GaInAsSb lasers and GaInNAsSb lasers, respectively. Here, note that the Ith for lasers with HR coatings (CL/HR, HR/HR) agrees well with the theoretical curves.

The temperature dependence of light output power against injected current (L–I) characteristics was investigated for lasers ($L = 300$ μm, CL/95%) at pulse conditions, as shown in Fig. 13(a) for GaInAsSb lasers and Fig. 13(b) for GaInNAsSb lasers. The slope efficiencies at 25 °C were 0.46 W/A for GaInAsSb and 0.44 W/A for GaInNAsSb lasers. The maximum oscillating temperatures were 145 °C for GaInAsSb and 95 °C for GaInNAsSb lasers. Fig. 14 shows the temperature

TABLE I
ESTIMATED LASER PARAMETERS FOR GaInAsSb–SQW LASERS AND GaInNAsSb–SQW LASERS

Device type	ξ_w	G_0 (cm^{-1})	Jtr/η (A/cm^2)	α_i (cm^{-1})	η_i
GaInAsSb-SQW	0.0199	1450	150	7	1
GaInNAsSb-SQW	0.0198	1700	380	7	1

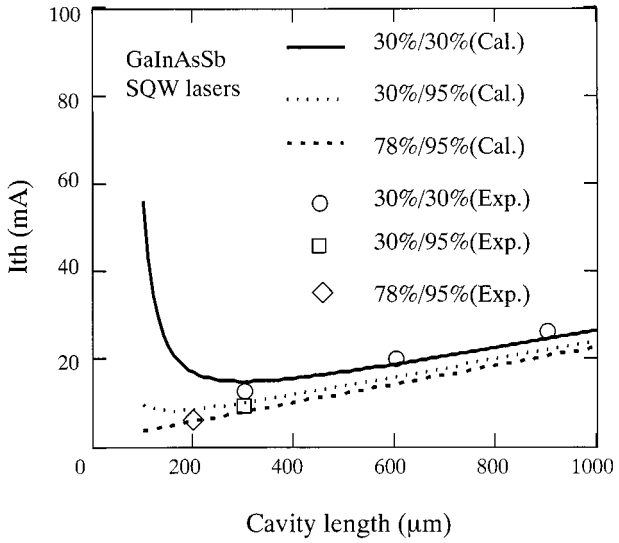

Fig. 11. Ith against cavity length for GaInAsSb–SQW lasers with a parameter of facet reflectivity. The lines are theoretical curves calculated by (5).

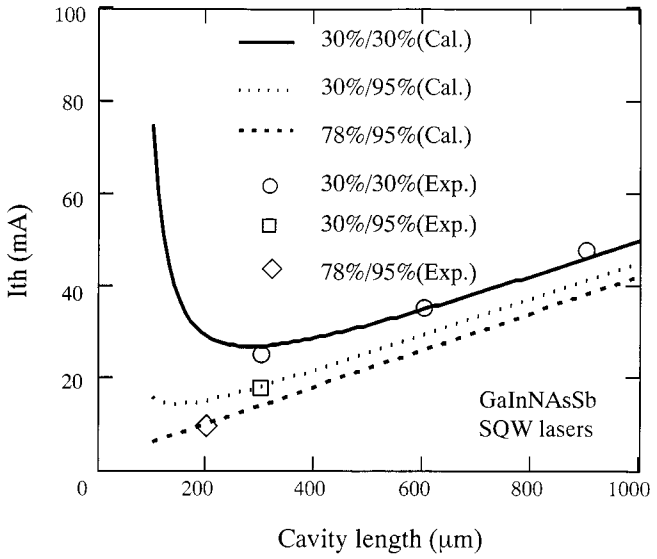

Fig. 12. Ith against cavity length for GaInNAsSb–SQW lasers with a parameter of facet reflectivity. The lines are theoretical curves calculated by (5).

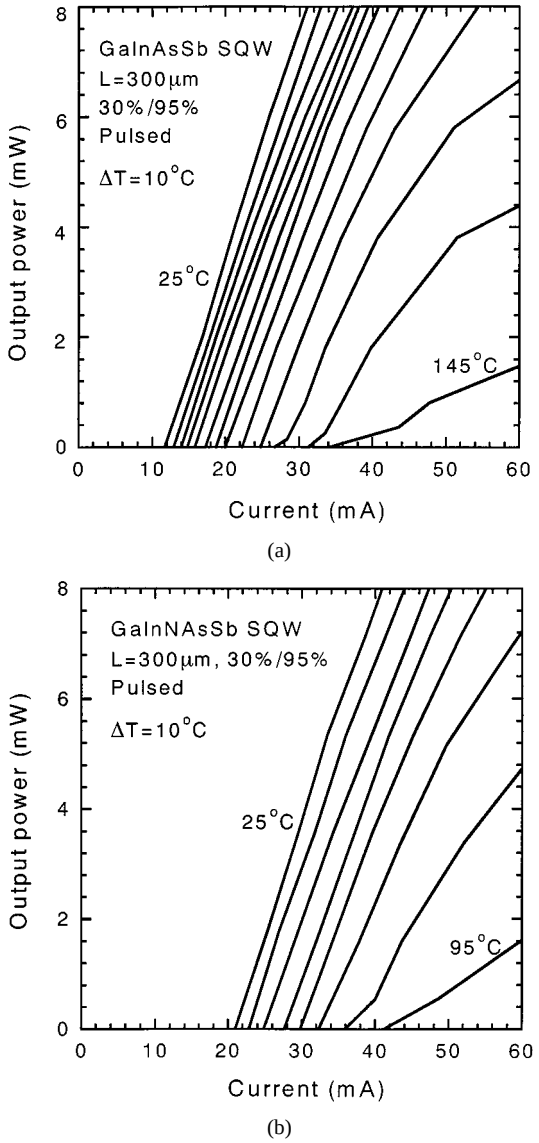

Fig. 13. The temperature dependence of light–current characteristics for (a) GaInAsSb lasers and (b) GaInNAsSb lasers under pulsed operation ($L = 300$ μm, 30/95%).

dependence of Ith for these lasers, where we can see that the characteristic temperatures are 120 K (at 25–125 °C) for GaInAsSb lasers and 111 K (at 25–85 °C) for GaInNAsSb lasers. Fig. 15 shows the temperature dependence of the maximum slope efficiencies for these lasers. The decreasing rate of the maximum slope efficiencies was −0.010 dB/K (at 25–125 °C) for GaInAsSb and −0.022 dB/K (at 25–75 °C) for GaInNAsSb lasers. Although the band offset for the electron becomes larger by adding N into the well, the temperature

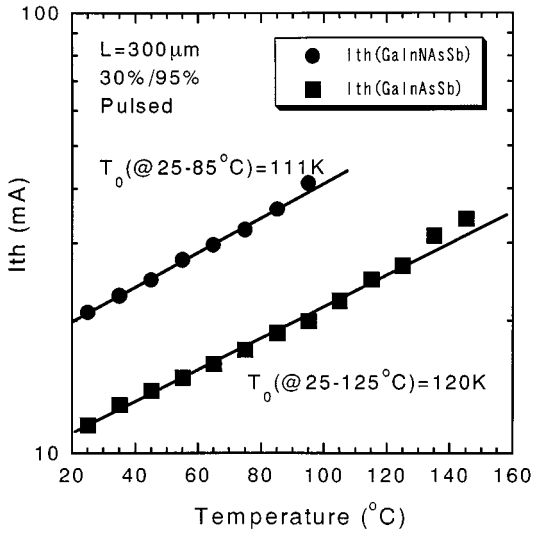

Fig. 14. The temperature dependence of the threshold currents for GaInAsSb and GaInNAsSb–SQW lasers under pulsed operation ($L = 300$ μm, 30/95%).

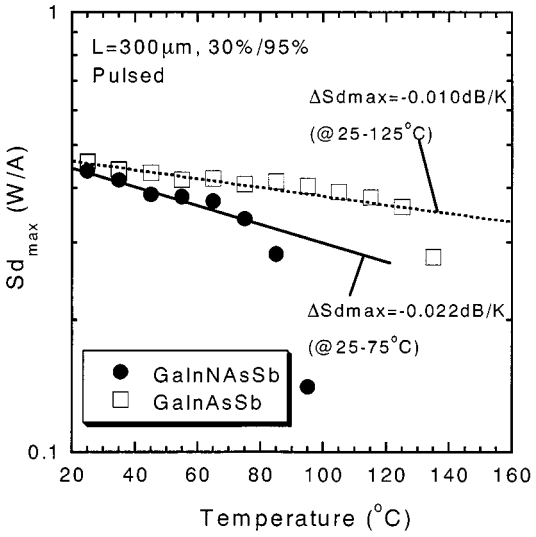

Fig. 15. The temperature dependence of the slope efficiency for GaInAsSb and GaInNAsSb–SQW lasers under pulse operation ($L = 300$ μm, 30/95%).

dependence of L–I curves of GaInNAsSb lasers deteriorated compared with GaInAsSb lasers. This could be due to the poor crystalline of GaInNAsSb lasers; therefore, further improvement can be expected by optimizing growth conditions of GaInNAsSb–SQW layers.

B. DC Characteristics of Ridge Lasers

The short cavity lasers ($L = 200$ μm) with high reflection (HR) coatings on both facets ($R_f/R_r = 78\%/95\%$) were tested under CW operation. Fig. 16 shows the temperature dependence of light-current characteristics for GaInNAsSb lasers. The low Ith of 12.4 mA at 25 °C was obtained under CW operation, which is the almost the same value with the best results ever reported for narrow stripe lasers [6]. The lasing wavelength is 1.258 μm as shown in the inset of Fig. 16. Large T_0 of 157 K was obtained in the range of 25–85 °C; therefore, this is the best result for GaInNAs-based edge emission lasers with the low Ith

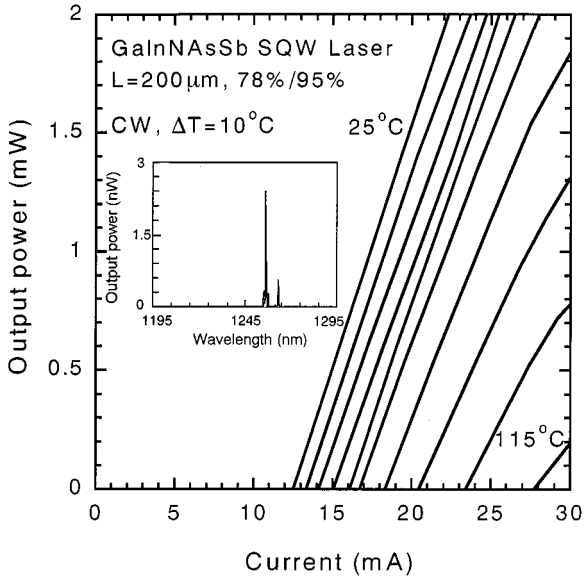

Fig. 16. The temperature dependence of light–current characteristics for GaInNAsSb lasers under CW operation ($L = 200$ μm, 78/95%). The inset shows lasing spectrum at room temperature.

and the large T_0 to our best knowledge [5], [6]. Furthermore, the relatively high slope efficiency of 0.22 W/A at 25 °C, the superior decreasing rate of the maximum slope efficiency of −0.014 dB/K (at 25–85 °C) and the CW oscillating at more than 100 °C were obtained. GaInAsSb lasers ($L = 200$ μm, 78/95%) were also tested under CW operation. The lasing wavelength of GaInAsSb laser is 1.20 μm at 20 °C, and the lasers show lower Ith (6.3 mA at 20 °C) and higher T_0 (256 K at 20–70 °C) [26] as compared with GaInNAsSb lasers, and it is also the best result for the 1.2-μm-range highly strained GaInAs-based narrow stripe lasers [10], [26]. From these results, we can say that GaInNAsSb QF lasers are very promising material for realizing pertier-free access network.

Further, the relaxation oscillation frequency was measured from the relative intensity noise (RIN) spectrum for 200-μm-long devices with HR coatings on both facets (78%/95%) in order to estimate the differential gain. The output power dependence of the RIN spectrum of GaInNAsSb–SQW lasers is shown in Fig. 17.

Fig. 18 shows the square of the relaxation oscillation frequency against the output power from the front facet. The efficiency of the relaxation frequency for GaInNAsSb–SQW lasers is 3.25 GHz/(mW)$^{1/2}$, which is comparable to the reported value of 3.25 GHz/(mW)$^{1/2}$ in 980-nm GaInAs–AlGaAs–SQW lasers [27]. The relaxation oscillation frequency can be described as follows:

$$fr = \frac{1}{2\pi}\sqrt{\frac{S_0 \Gamma g_0 v_g}{\tau_p}} \tag{6}$$

where

S_0 photon density in the QW layer;
Γ optical confinement factor;
g_0 differential gain;
V_g group velocity;
τ_p photon lifetime.

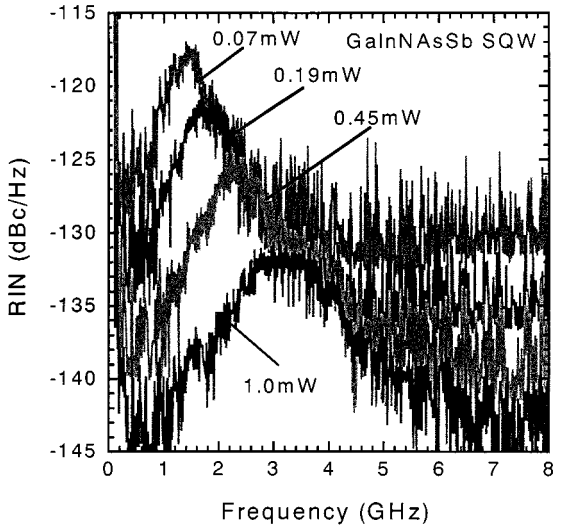

Fig. 17. The output power dependence of RIN spectrum of GaInNAsSb–SQW lasers.

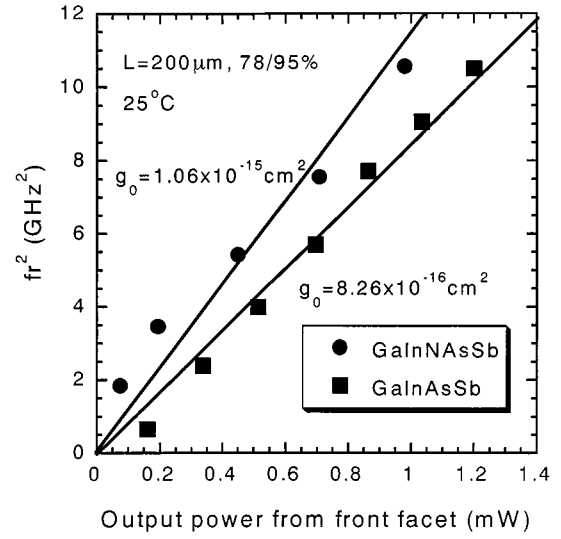

Fig. 18. The square of the relaxation oscillation frequency against output power from the front facet.

The relationship between S_0 and the output power from the both facets ($P_{\rm both}$) can be described as follows:

$$P_{\rm both} = P_f + P_r = \frac{1}{\tau_p}\left(\frac{\alpha_m}{\alpha_m + \alpha_i}\right) h\nu V S_0 \tag{7}$$

where

P_f output power from the front facet;
P_r output power from the rear facet;
α_m mirror loss;
$h\nu$ photon energy;
V volume of the QW layer.

P_f/P_r can be described as follows:

$$\frac{P_f}{P_r} = \frac{1-R_f}{1-R_r}\sqrt{\frac{R_r}{R_f}}. \tag{8}$$

Further, τ_p can be expressed as follows:

$$\frac{1}{\tau_p} = v_g(\alpha_i + \alpha_m). \tag{9}$$

From (6) to (9), we can get the relationship between f_r^2 and P_f as follows:

$$f_r^2 = \frac{g_0 \Gamma v_g}{4\pi^2 V h\nu}\left(\frac{\alpha_i + \alpha_m}{\alpha_m}\right)\left[1 + \left(\frac{R_r}{R_f}\right)^{-1/2}\left(\frac{1-R_r}{1-R_f}\right)\right] P_f. \tag{10}$$

The differential gain was determined from the slope in Fig. 18 using (10). The extremely large differential gain of 1.06×10^{-15} cm^2 for 1.26-μm-GaInNAsSb–SQW lasers and 8.26×10^{-16} cm^2 for 1.20-μm-GaInAsSb–SQW lasers were estimated, respectively. This is the first report for the differential gain in GaInNAs-based lasers and 1.2-μm-range GaInAs-based QF lasers to the best of our best knowledge. The differential gain of GaInNAsSb lasers was enhanced by a factor of 1.28 as compared with GaInAsSb lasers, which agrees well with the enhancement of G_0 by a factor of about 1.20 between these lasers, which is probably due to the strong electron confinement by deeper band offset for electrons by adding N. The reported differential gain in 980 nm InGaAs–AlGaAs–SQW lasers was about 7×10^{-16} cm^2 [27]; therefore, the larger differential gain as compared with 980-nm InGaAs–AlGaAs–SQW lasers is attributed to the deeper band offset for electrons by increasing indium composition and adding N. The differential gain of a GaInNAsSb–SQW laser is much larger than that of long-wavelength compressively strained GaInAsP–4QW lasers ($g_0 = 2.5 \times 10^{-16}$ cm^2) [28] or InAsP–3QW lasers ($g_0 = 1.7 \times 10^{-16}$ cm^2) [29] and is still larger than that of the strain-compensated GaInAsP–16QW lasers (6 to 7×10^{-16} cm^2) [30].

From these results, we can say that GaInNAsSb lasers are also suitable for high-speed lasers in the long wavelength region, and the higher modulation response can be expected by increasing the number of the well.

IV. Conclusion

Long wavelength GaInNAsSb and GaInAsSb–SQW lasers, that include the small amount of Sb, were successfully grown on GaAs substrates by GSMBE. We confirmed that Sb reacts in a highly strained GaInAs–GaAs system and a GaInNAs–GaAs system like a surfactant, which increases the critical thickness at which the growth mode changes from 2-D growth to 3-D growth. Low CW Ith (12.4 mA) with high T_0 (157 K) and over 100 °C oscillation was obtained for 1.26-μm GaInNAsSb–SQW ridge lasers and low CW Ith (6.3 mA) with high T_0 (256 K) was obtained for 1.20-μm GaInAsSb–SQW ridge lasers. Both types of lasers are the best results ever reported for GaInNAs-based edge emission lasers and highly strained GaInAs-based edge emission lasers with low Ith and high T_0 to the best of our knowledge. GaInNAsSb–QF lasers are very promising material for realizing peltier-free access network. Further, we think that GaInNAsSb lasers are suitable for high-speed lasers in the long

wavelength region because these lasers have the very large differential gain in spite of the single-QW.

ACKNOWLEDGMENT

The authors would like to thank J. Kikawa for his encouragement through this study. They also acknowledge Assistant Professor T. Miyamoto and T. Kageyama of Tokyo Institute of Technology for their kind advice for the N radical cell. Further, we also acknowledge Dr. M. Yokozeki, Dr. S. Yoshida, Dr. Y. Hiratani, and T. Kurobe for their helpful discussions for RF-GSMBE growth.

REFERENCES

[1] M. Kondow, S. Nakatsuka, T. Kitatani, Y. Yazawa, and M. Okai, "Room-temperature pulsed operation of GaInNA's laser diodes with excellent high-temperature performance," *Jpn. J. Appl. Phys.*, vol. 35, pp. 5711–5713, 1996.

[2] K. Nakahara, M. Kondow, T. Kitatani, M. C. Larson, and K. Uomi, "1.3-μm continuous-wave lasing operation in GaInNA's quantum-well lasers," *IEEE Photon. Technol. Lett.*, vol. 10, pp. 487–488, 1998.

[3] S. Sato and S. Satoh, "Room-temperature continuous-wave operation of 1.24-μm GaInNA's lasers grown by metal–organic chemical vapor deposition," *IEEE J. Select. Topics Quantum Electron.*, vol. 5, pp. 707–710, 1999.

[4] S. Sato and S. Satoh, "High-temperature characteristic in 1.3-μm-range highly strained GaInNA's ridge lasers grown by metal–organic chemical vapor deposition," *IEEE Photon. Technol. Lett.*, vol. 11, pp. 1560–1562, 1999.

[5] B. Borchert, A. Y. Egorov, S. Illek, M. Komainda, and H. Riechert, "1.29μm GaInNA's multiple quantum-well ridge-waveguide laser diodes with improved performance," *Electron. Lett.*, vol. 35, pp. 2204–2206, 1999.

[6] S. Illek, A. Ultsch, B. Borchert, A. Y. Egorov, and H. Riechert, "Low threshold lasing operation of narrow stripe oxide-confined GaInNAs/GaAs multiquantum well lasers at 1.28μm," *Electron. Lett.*, vol. 36, pp. 725–726, 2000.

[7] T. Kageyama, T. Miyamoto, S. Makino, N. Nishiyama, F. Koyama, and K. Iga, "High-temperature operation up to 170°C of GaInNAs–GaAs quantum-well lasers grown by chemical beam epitaxy," *IEEE Photon. Technol. Lett.*, vol. 12, pp. 10–12, 2000.

[8] X. Yang, M. J. Jurkovic, J. B. Heroux, and W. I. Wang, "Low threshold InGaAsN/GaAs single quantum well lasers grown by molecular beam epitaxy using Sb surfactant," *Electron. Lett.*, vol. 35, pp. 1082–1083, 1999.

[9] D. A. Livshits, A. Y. Egorov, and H. Riechert, "8W continuous wave operation of InGaAsN lasers at 1.3μm," *Electron. Lett.*, vol. 36, pp. 1381–1382, 2000.

[10] F. Koyama, D. Schlenker, T. Miyamoto, Z. Chen, A. Matsutani, T. Sakaguchi, and K. Iga, "Data transmission over single-mode fiber by using 1.2-μm uncooled GaInAs–GaAs laser for Gb/s local area network," *IEEE Photon. Technol. Lett.*, vol. 12, pp. 125–127, 2000.

[11] D. Schlenker, T. Miyamoto, Z. Chen, F. Koyama, and K. Iga, "Growth of highly strained GaInAs/GaAs quantum wells for 1.2μm wavelength lasers," *J. Crystal Growth*, vol. 209, pp. 27–36, 2000.

[12] W. J. Choi, P. D. Dapkus, and J. J. Jewell, "1.2-μm GaAsP/InGaAs strain compensated single-quantum-well diode laser on GaAs using metal–organic chemical vapor deposition," *IEEE Photon. Technol. Lett.*, vol. 11, pp. 1572–1574, 1999.

[13] M. Yamada, T. Anan, K. Tokutome, K. Nishi, A. Gomyo, and S. Sugou, "Low threshold lasing at 1.3μm from GaAsSb quantum wells directly grown on GaAs substrates," in *Conf. Proc. LEOS'98*, Orlando, FL, 1998, Paper WA3, pp. 149–150.

[14] X. Huang, A. Stintz, C. P. Hains, G. T. Liu, J. Cheng, and K. J. Malloy, "Efficient high-temperature CW lasing operation of oxide-confined long-wavelength InAs quantum dot lasers," *Electron. Lett.*, vol. 36, pp. 41–42, 2000.

[15] K. Mukai, Y. Nakata, K. Otsubo, M. Sugawara, N. Yokoyama, and H. Ishikawa, "1.3-μm CW lasing of InGaAs–GaAs quantum dots at room temperature with a threshold current of 8mA," *IEEE Photon. Technol. Lett.*, vol. 11, pp. 1205–1207, 1999.

[16] K. D. Choquette, K. M. Geib, C. H. Ashby, R. D. Twesten, O. Blum, H. Q. Hou, D. M. Follstaedt, B. E. Hammons, D. Mathes, and R. Hull, "Advances in selective wet oxidation of AlGaAs alloys," *IEEE J. Select. Topics Quantum Electron.*, vol. 3, pp. 916–926, 1997.

[17] M. Kudo and T. Mishima, "Improved photoluminescence properties of highly strained InGaAs/GaAs quantum wells grown by molecular-beam epitaxy," *J. Appl. Phys.*, vol. 78, pp. 1685–1688, 1995.

[18] D. E. Mars, D. I. Babic, Y. Kaneko, and Y. L. Chang, "Growth of 1.3μm InGaAsN laser material on GaAs by molecular beam epitaxy," *J. Vac. Sci. Technol. B*, vol. 17, pp. 1272–1275, 1999.

[19] M. Copel, M. C. Reuter, E. Kaxiras, and R. M. Tromp, "Surfactants in epitaxial growth," *Phys. Rev. Lett.*, vol. 63, pp. 632–635, 1989.

[20] N. Grandjean, J. Massies, and V. H. Etgens, "Delayed relaxation by surfactant action in highly strained III–V semiconductor epitaxial layer," *Phys. Rev. Lett.*, vol. 69, pp. 796–799, 1992.

[21] H. Shimizu, K. Kumada, S. Uchiyama, and A. Kasukawa, "1.2μm-range GaInAs SQW lasers using Sb as surfactant," *Electron. Lett.*, vol. 36, pp. 1379–1381, 2000.

[22] J. W. Matthews and A. E. Blakeslee, "Defects in epitaxial multilayers," *J. Crystal Growth*, vol. 27, pp. 118–125, 1974.

[23] O. Madelung, *Landolt–Bornstein in Numerical Data and Functional Relationships in Science and Technology*, ser. new series III: Springer-Verlag, 1982, vol. 17 and 22a.

[24] J. S. Osinski, P. Grodzinski, Y. Zou, and P. D. Dapkus, "Threshold current analysis of compressive strain (0–1.8%) in low-threshold, long-wavelength quantum well lasers," *IEEE J. Quantum Electron.*, vol. 29, pp. 1576–1585, 1993.

[25] S. Y. Hu, D. B. Young, A. C. Gossard, and L. A. Coldren, "The effect of lateral leakege current on the experimental gain/current–density curve in quantum-well ridge-waveguide lasers," *IEEE J. Quantum Electron.*, vol. 30, pp. 2245–2250, 1994.

[26] H. Shimizu, K. Kumada, S. Uchiyama, and A. Kasukawa, "High performance CW 1.26μm GaInNAsSb-SQW and 1.20μm GaInAsSb-SQW ridge lasers," Electron. Lett., vol. 36, 2000, to be published.

[27] R. Nagarajan, T. Fukushima, M. Ishikawa, J. E. Bowers, R. S. Geels, and L. A. Coldren, " Transport limits in high-speed quantum-well lasers: Experiment and theory," *IEEE Photon. Technol. Lett.*, vol. 4, pp. 121–123, 1992.

[28] Y. Zou, J. S. Osinski, P. Grodzinski, P. D. Dapkus, W. C. Rideout, W. F. Sharfin, J. Schlafer, and F. D. Crawford, "Experimental study of Auger recombination, gain, and temperature sensitivity of 1.5μm compressively strained semiconductor lasers," *IEEE J. Quantum Electron.*, vol. 29, pp. 1565–1575, 1993.

[29] H. Shimizu, K. Kumada, N. Yamanaka, N. Iwai, T. Mukaihara, and A. Kasukawa, "1.3-μm InAsP modulation-doped MQW lasers," *IEEE J. Quantum Electron.*, vol. 36, pp. 728–735, 2000.

[30] M. C. Tatham, C. P. Seltzer, S. D. Perrin, and D. M. Cooper, "Frequency response and differential gain in strained and unstrained InGaAs/InGaAsP quantum well lasers," *Electron. Lett.*, vol. 27, pp. 1278–1280, 1991.

Hitoshi Shimizu was born in Yamanashi Prefecture, Japan, in 1966. He received the B.S. degree in physical engineering from Tokyo University, Tokyo, Japan, in 1989.

In 1989, he joined the Furukawa Electric Co., Ltd., at Yokohama Research and Development Laboratories, Yokohama, Japan. He was engaged in research on quantum-well lasers in GaInAs–AlGaAs, AlGaInAs–InP material systems by molecular-beam epitaxy growth, and the modulation doped quantum-well lasers in InAsP–InP material systems by gas-source molecular-beam epitaxy growth. He is currently interested in the highly strained GaInNA's quantum-well lasers and its applications. He holds four U.S. patents.

Mr. Shimizu is a member of the Japan Society of Applied Physics.

Kouji Kumada was born in Kanagawa Prefecture, Japan, in 1965.

He jointed the Furukawa Electric Co., Ltd., Yokohama Research and Development Laboratories, Yokohama, Japan, where he studied the bulk crystal of GaAs by liquid encapsulated Czochralski method. His current research interests include long-wavelength strained quantum-well lasers grown by gas-source molecular-beam epitaxy.

Seiji Uchiyana (M'87)was born in Saitama Prefecture, Japan, in 1958. He received the B.E., M.E., and Dr.Eng. degrees from Tokyo Institute of Technology, Japan, in 1981, 1983, and 1986, respectively.

From 1986 to 1992, he was with the Department of Image Science and Engineering, Chiba University. From 1990 to 1991, he spent one year as a Postdoctoral MTS at Crawford Hill Laboratory, AT&T Bell Laboratories, Holmdel, NJ. In 1992, he joined The Furukawa Electric Co., Ltd., Yokohama, Japan, where he has been engaged in the research and development of VCSEL.

Dr. Uchiyama is a member of Institute of Electronics, Information and Communication Engineers (IEICE) of Japan, the Japan Society of Applied Physics, and the Optical Society of Japan.

Akihiko Kasukawa (A'94) was born in 1958. He received the B.S., M.S., and Ph.D. degrees in electrical engineering all from Tokyo Institute of Technology, Tokyo, Japan, in 1982, 1984, and 1994.

In 1984, he joined The Furukawa Electric Company, Ltd., Yokohama, Japan. At Furukawa, he has been engaged in research and development of long-wavelength semiconductor lasers. From 1990 to 1991, he spent one year at Bell Communication Research (Bellcore) Inc., Red Bank, NJ, as a Visiting Researcher. After coming back to Furukawa Electric, Yokohama R&D Laboratories, he conducted the development of long-wavelength strained-layer quantum-well lasers. In 1994, he received the Technology award from Fiber Optic Products News for high-power 1480-nm pumping laser modules for EDFA. His research includes the first room-temperature pulsed operation of 1.5-μm VCSELs in 1989, first demonstration of low-threshold-current density 1.3- and 1.5-μm GRIN-SCH quantum-well lasers in 1989, the novel InAsP–InP lasers in 1992. He is an author and co-author of 90 technical papers and conference papers, and co-author of one book chapter. He holds three U.S. patents. His current research interests include high-power pumps (980 and 1480 nm) ultralow-threshold lasers, optical devices for access networks, and epitaxial growth.

Dr. Kasukawa is a member of the Japanese Society of Applied Physics (JSAP) and the Institute of Electronics, Information and Communication Engineers (IEICE) of Japan.